APPLICATION OF HYBRID AERO-ENGINE MODEL FOR INTEGRATED FLIGHT/PROPULSION OPTIMAL CONTROL

Wang Jiankang, Zhang Haibo, Sun Jianguo, Li Yongjin

(College of Energy and Power Engineering, Nanjing University of Aeronautics and Astronautics, Nanjing, 210016, P. R. China)

Abstract: The real-time capability of integrated flight/propulsion optimal control (IFPOC) is studied. An application is proposed for IFPOC by combining the onboard hybrid aero-engine model with sequential quadratic programming (SQP). Firstly, a steady-state hybrid aero-engine model is designed in the whole flight envelope with a dramatic enhancement of real-time capability. Secondly, the aero-engine performance seeking control including the maximum thrust mode and the minimum fuel-consumption mode is performed by SQP. Finally, digital simulations for cruise and accelerating flight are carried out. Results show that the proposed method improves real-time capability considerably with satisfactory effectiveness of optimization.

Key words: integrated flight/propulsion optimal control; aero-engine; hybrid model; performance seeking control; sequential quadratic programming

CLC number: V231 **Document code**: A **Article ID**: 1005-1120(2012)01-0016-09

Nomenclature

A_8 m^2 Nozzle throat area

d_{Gvf}/(°) Fan inlet variable guide vane angle

d_{Gvc}/(°) Compressor inlet variable guide vane angle

F/N Net thrust

H/km Flight altitude

Ma Flight Mach number

P/Pa Total pressure at specified engine station number

Pla/(°) Power lever angle

PNF/% Fan rotor speed

PNC/% Core rotor speed

sfc/(kg · h^{-1} · N^{-1}) Specific fuel consumption

SMf Fan stall margin

SMc Compressor stall margin

T/K Total temperature at specified engine station number

V/(m · s^{-1}) Flight velocity

W_{fa}/(kg · s^{-1}) Afterburner fuel flow rate

W_{fb}/(kg · s^{-1}) Fuel flow rate

WA_{22C}/(kg · s^{-1}) Fan outlet corrected airflow

WA_{25C}/(kg · s^{-1}) Compressor inlet corrected airflow

α/(°) Angle of attack

π_T Pressure ratio of turbine

Suffixes (aero-engine station numbers)

0 Free stream

2 Fan inlet

25 Compressor inlet

4 Main combustion outlet

45 Low-pressure turbine inlet

46 Low-pressure turbine outlet

7 Afterburner inlet

75 Afterburner outlet

8 Nozzle throat area

INTRODUCTION

The integrated flight/propulsion optimal control (IFPOC)[1-2] is to control the integrated system by aero-engine performance seeking control (PSC)[2-4]. As the heart of IFPOC, PSC contains the following optimization modes: maximum thrust mode, minimum fuel-consumption mode and minimum turbine temperature mode. PSC en-

Foundation items: Supported by the Aeronautical Science Foundation of China (2010ZB52011); the Funding of Jiangsu Innovation Program for Graduate Education(CXLX11-0213);the Nanjing University of Aeronautics and Astronautics Research Funding (NS2010055).

Received date: 2010-10-27; **revision received date**: 2011-06-03

E-mail: wangjiankang16@163.com

ables the aero-engine to achieve its full potential and improves aircraft flight performance. In 1990s, National Aeronautics and Space Administration and US Air Force conducted a large number of PSC flight tests[5-6]. The results[6] proved that PSC could significantly improve aero-engine performance and the flexibility, mobility and economical efficiency of aircraft.

The conventional optimization adopts linear programming (LP) to optimize the integrated model based on nonlinear aero-engine model. In Ref. [7], sequential quadratic programming (SQP) is applied to PSC successfully for the first time with a better optimization accuracy. However, the real-time capability of optimization is about 6 s, which can not meet the requirement in practical application.

Considering the large time-cost of iterative calculations during optimization[7], it is necessary to simplify the nonlinear aero-engine model to improve real-time ability. Therefore, propulsion system matrix (PSM) is introduced based on similarity parameters. The simplified model has two merits: real-time capability enhancement through linearizing models for most aero-engine components, and accuracy improvement by nonlinear models for some engine components. The geometrical dissimilarities of several components including nozzle are also considered during optimizing aero-engine. In this way, a hybrid aero-engine model is built in the whole flight envelop.

Finally, the approach of IFPOC is presented based on the hybrid aero-engine model and SQP. Digital simulations are conducted for cruise and accelerating flight. Results demonstrate that flight performance is further improved with good real-time ability of optimization.

1 ONBOARD HYBRID AERO-ENGINE MODEL

1.1 Design of hybrid aero-engine model

The object of the study is a dual-spool afterburning turbofan engine with mixed exhaust. To simplify the nonlinear aero-engine model in the whole flight envelope, the ground and non-ground state of aero-engine need to be set interconvertible based on similarity theory[8]. For this, aero-engine must satisfy the conditions of geometric, kinematic and dynamic similarity. But the number of linear engine models grows exponentially with the increase of similarity conditions. Because the engine has many adjustable parameters, including inlet ramp angle, fan inlet variable guide vanes angle, compressor inlet variable guide vane angle, nozzle throat area, it is difficult to build the hybrid engine model in the full envelop. Reducing similarity conditions is therefore necessary.

Similarity conditions are reduced in three main aspects. First, after considering possible shift of inlet ramp during supersonic flight, the inlet is separated from the engine and calculated alone so that the similarity condition of inlet can be ignored. Second, d_{Gvf} and d_{Gvc} are always changed slightly during optimization. Thus the influences of d_{Gvf} and d_{Gvc} on similarity are little and can be ignored. Third, the nozzle throat area needs to be adjusted during afterburning or optimizing. Consequently the engine can not meet the similarity condition. Segregating afterburner and nozzle components from the engine is adopted to solve this problem.

The hybrid aero-engine model is proposed by block partition of components based on the above analyses. On one hand, because components from fan to mixer can meet the similarity conditions under all flight conditions, the models of these components are established with linear method and extended to the whole envelope based on similarity theory. Therefore real-time ability is improved markedly. On the other hand, components including inlet, afterburner and nozzle sometimes can not meet the similarity conditions. Their models are built by nonlinear method to improve the model accuracy.

1.2 Linear steady-state aero-engine model

Linear aero-engine model is used for aerothermodynamics calculation from fan to mixer. Using linearization within a linear range of every small flight envelope, the functional relation between the engine control variable and the state variable is determined and mathematically expressed as

$$\Delta y_i = \sum_j (P_{ij} \cdot \Delta u_j) \tag{1}$$

where $\Delta y_i = \dfrac{y_i - y_{i0}}{y_{id}}$, $\Delta u_j = u_j - u_{j0}$, P_{ij} represents PSM matrix element, u_j and y_i represent the engine control variable and the state, respectively, u_{j0} and y_{i0} the initial steady-state value of control variable and the state variable, respectively, and y_{id} represents the value of state variable in the design point.

Set the engine control variable $\boldsymbol{u} = [A_8, W_{fb}, W_{fa}, d_{Gvf}, d_{Gvc}]^T$ and the engine state variable $\boldsymbol{y} = [PNC, PNF, P_{25}, P_4, P_7, T_{25}, T_{45}, T_7, WA_{22C}, WA_{25C}]^T$. The hybrid model is built under non-afterburning condition as well as afterburning condition.

In non-afterburning condition, if combustor inlet corrected pressure P_{3cor} and mixer inlet corrected pressure P_{6cor} are established, the state of aero-engine will be determined. The steps of obtaining PSM are as follows:

(1) P_{3cor} and P_{6cor} are divided by two-dimensional average segmentation in the standard atmosphere.

(2) The number of the engine operation points for the computation of PSM is defined (66 operation points in all).

(3) Twin-variable augmented linear quadratic regulator (LQR) controller[9] is designed to get the inputs of engine model.

(4) PSM is computed with the above engine operation points.

(5) Linear engine sub-models are all established in non-afterburning condition on the ground.

In afterburning condition, if a change of W_{fa} occurs, π_T will be altered. In closed loop system, A_8 is adjusted accordingly to keep π_T unchanged by the afterburning controller. That is, A_8 is fixed with the affirmation of W_{fa}. The state of engine can be decided by W_{fa} only. The method of gaining PSM follows the steps as:

(1) W_{fa} is divided by one-dimensional average segmentation on the ground.

(2) The number of engine operation points is ensured as 30 in all.

(3) After the closed-loop engine system running, the open-loop control is switched on to compute PSM with the above operation points.

(4) Linear engine sub-models are all built in afterburning condition on the ground.

That all of linear engine sub-models are built on the ground can cover all operation points in the whole envelope using similarity transformation (Fig. 1). In Fig. 1, old engine operating point is calculated from nonlinear engine model, and new engine operating point is determined by PSM.

1.3 Nonlinear steady-state aero-engine model

Nonlinear steady-state model is to calculate the components and parameters not suitable for similarity theory, including inlet, afterburner, nozzle, fan stall margin and compressor stall margin.

The inlet nonlinear model is expressed as

$$[T_2, P_2, V_0, P_0]^T = f_{inlet}(\theta, PNFc) \tag{2}$$

where $\theta = [H, Ma, \alpha]^T$ represents flight parameter, and $PNFc$ the fan rotor corrected speed.

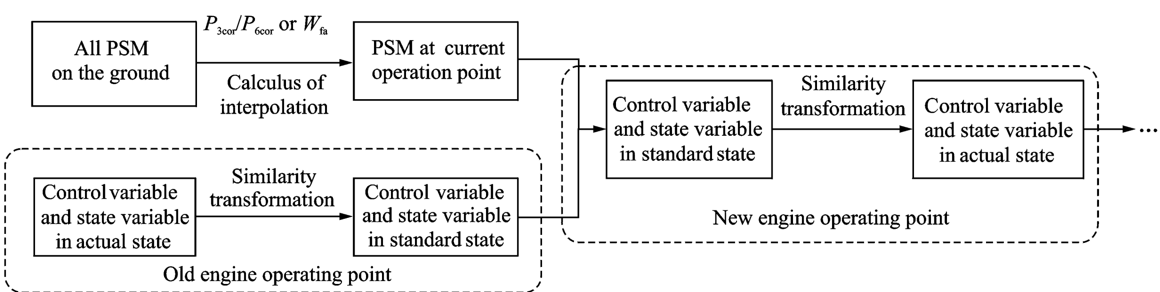

Fig. 1 Realization of linear model in whole envelope

According to the outputs of linear model, the afterburner nonlinear model is built by calculating component characteristics and equilibrium equations. The model is represented as

$$[P_{75}, T_{75}, WG_{75}]^{\mathrm{T}} = f_{\text{afterburner}}(W_{\text{fb}}, W_{\text{fa}}, WA_{22\text{C}}, WA_{25\text{C}}, T_7, P_7) \quad (3)$$

The nozzle nonlinear model is built as

$$[P_8, T_8, WG_8, V_8]^{\mathrm{T}} = f_{\text{nozzle}}(W_{\text{fb}}, W_{\text{fa}}, WG_{75}, P_{75}, T_{75}, P_0) \quad (4)$$

Besides, SMf and SMc depend on engine's characteristic lines and working spots on those lines[10]. Because the change of fan and compressor variable vane angle will influence characteristic lines and operation point location, the control laws and total characteristic data of fan and compressor variable vane angle are ported to the hybrid engine model. SMf and SMc are expressed as

$$SMf = f_{\text{smf}}(d_{\text{Gvf}}, PNF, T_2, P_2, P_{25}, WA_{22\text{C}}) \quad (5)$$

$$SMc = f_{\text{smc}}(d_{\text{Gvc}}, PNC, T_{25}, P_{25}, P_4, WA_{25\text{C}}) \quad (6)$$

1.4 Hybrid aero-engine model

Based on the above analysis, the hybrid aero-engine model is established by Eqs. (1-6). The thrust and specific fuel consumption of aero-engine are expressed as

$$F = WG_8 \cdot V_8 - WA_2 \cdot V_0 + (P_8 - P_0) \cdot A_8$$

$$sfc = 3\,600 \cdot (W_{\text{fb}} + W_{\text{fa}})/F$$

that is

$$[F, sfc]^{\mathrm{T}} = f_{\text{thrust}}(W_{\text{fb}}, W_{\text{fa}}, P_8, V_8, WA_{22\text{C}}, WA_{25\text{C}}, A_8, P_0) \quad (7)$$

Summarily the hybrid aero-engine model is described as

$$\boldsymbol{Y}_{\text{engine}} = f_{\text{engine}}(\theta, \boldsymbol{u}, \boldsymbol{y}) \quad (8)$$

where $\boldsymbol{Y}_{\text{engine}} = [F, sfc, SMf, SMc, PNF, PNC, T_{46}]^{\mathrm{T}}$ represents the engine model output, $\theta = [H, Ma, \alpha]^{\mathrm{T}}$ the flight parameter, $\boldsymbol{u} = [A_8, W_{\text{fb}}, W_{\text{fa}}, d_{\text{Gvf}}, d_{\text{Gvc}}]^{\mathrm{T}}$ the control variable, and $\boldsymbol{y} = [PNF, PNC, P_2, P_{25}, P_3, P_4, P_6, P_7, T_{25}, T_{45}, T_7, WA_{22\text{C}}, WA_{25\text{C}}]^{\mathrm{T}}$ the input of linear model. The realization of the hybrid aero-engine model in the whole flight envelope is shown in Fig. 2.

In order to check the accuracy of hybrid aero-engine model, a small steps are added to all control variables to carry out simulations separately. Table 1 lists the accuracy of cruise operation point, $H=12$ km, $Ma=0.8$, $Pla=40°$. The accuracy while A_8 and W_{fa} being changed are listed in Tables 2-3, respectively. Tables 1-3 prove that the hybrid model has good accuracy.

In Tables 1-3, "a" represents the nonlinear aero-engine model, "b" the hybrid aero-engine model, and "$A_8(+1\%)$" adding 1% step to A_8, which is similar to the expression of other variables. Besides, the error e, thrust and specific fuel consumption are relative value and formulated as

$$e = \frac{x_{\text{b}} - x_{\text{a}}}{x_{\text{a0}}} \cdot 100\%, \quad Fr = \frac{F}{F_0} \cdot 100\%$$

$$sfcr = \frac{sfc}{sfc_0} \cdot 100\%$$

where x_{a} and x_{b} represent the parameter values of nonlinear model and hybrid model, respectively, and the subscript 0 identifies that the state is not optimized.

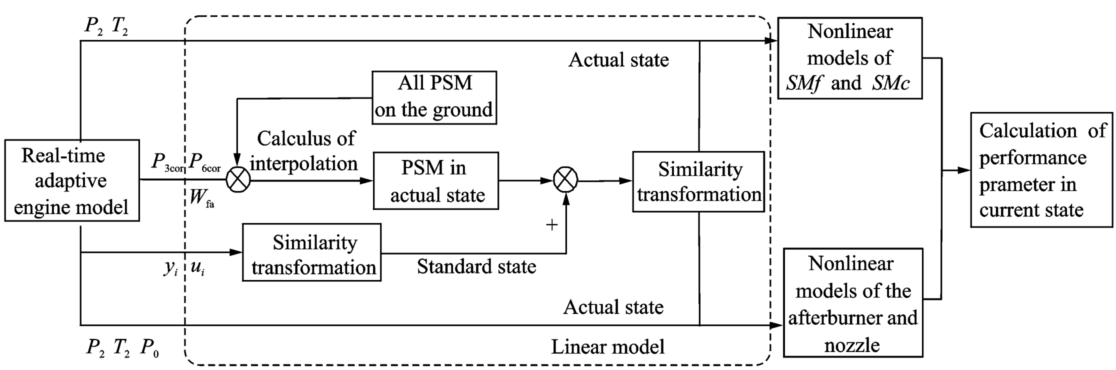

Fig. 2 Realization of hybrid model in whole flight envelope

Table 1 Accuracy at $H=12$ km, $Ma=0.8$, $Pla=40°$

Condition	Model	Fr	$sfcr$	SMf	SMc
No steps	a,b	1	1	0.277 54	0.191 20
$A_8(+1\%)$	a	1.000 72	0.999 29	0.293 54	0.190 92
	b	1.001 16	0.998 99	0.293 56	0.191 02
	Error	0.000 44	-3.00×10^{-4}	7.21×10^{-5}	5.23×10^{-4}
$W_{fb}(+1\%)$	a	1.010 18	0.999 71	0.277 64	0.191 22
	b	1.009 84	0.999 91	0.277 36	0.191 16
	Error	−0.000 34	2.00×10^{-4}	−0.001 01	-3.14×10^{-4}
$d_{Gvf}(-1)$	a	0.998 02	1.001 93	0.283 66	0.191 08
	b	0.998 17	1.001 59	0.283 61	0.191 11
	Error	0.000 15	-3.40×10^{-4}	-1.80×10^{-4}	1.57×10^{-4}
$d_{Gvc}(-1)$	a	0.998 17	1.001 76	0.275 62	0.195 28
	b	0.998 19	1.001 96	0.275 59	0.194 97
	Error	2.00×10^{-5}	2.00×10^{-4}	-1.08×10^{-4}	−0.001 62
$A_8(+1\%)$ $W_{fb}(+1\%)$	a	1.010 89	0.999 07	0.293 61	0.190 91
	b	1.011 09	0.998 68	0.293 29	0.190 98
	Error	0.000 20	-3.90×10^{-4}	−0.00115	3.66×10^{-4}
$A_8(+1\%)$ d_{Gvf}	a	0.998 72	1.001 18	0.299 86	0.190 76
	b	0.999 32	1.000 43	0.299 78	0.190 89
	Error	0.000 60	-7.50×10^{-4}	-2.88×10^{-4}	0.000 68
$A_8(+1\%)$ $d_{Gvc}(-1)$	a	0.998 86	1.001 08	0.291 59	0.194 95
	b	0.999 18	1.000 57	0.291 52	0.194 64
	Error	0.000 32	-5.10×10^{-4}	-2.52×10^{-4}	−0.001 62
$W_{fb}(+1\%)$ $d_{Gvf}(-1)$	a	1.008 21	1.001 59	0.283 85	0.191 07
	b	1.008 16	1.001 98	0.283 46	0.191 04
	Error	-5.00×10^{-5}	3.90×10^{-4}	−0.001 41	-1.57×10^{-4}
$W_{fb}(+1\%)$ $d_{Gvc}(-1)$	a	1.008 41	1.001 56	0.275 69	0.195 22
	b	1.008 16	1.001 96	0.275 42	0.194 88
	Error	−0.000 25	4.00×10^{-4}	−0.000 97	−0.001 78
$d_{Gvf}(-1)$ $d_{Gvc}(-1)$	a	0.996 24	1.003 71	0.281 69	0.195 07
	b	0.996 35	1.003 41	0.281 64	0.194 91
	Error	0.000 11	-3.00×10^{-4}	-1.80×10^{-4}	−0.000 83
Add steps to all	a	1.007 16	1.002 75	0.297 97	0.194 69
	b	1.007 56	1.002 18	0.297 61	0.194 56
	Error	0.000 4	-5.70×10^{-4}	−0.001 29	−0.000 68

Table 2 Accuracy while A_8 being changed at curse point

A_8/m^2	Condition	Model	Fr	$sfcr$	SMf	SMc
0.33	No steps	a, b	1	1	0.477 71	0.187 54
	Add steps to all	a	1.034 06	0.976 73	0.445 29	0.166 53
		b	1.034 08	0.976 71	0.445 62	0.166 47
		Error	2.00×10^{-5}	-2.00×10^{-5}	0.000 69	-3.20×10^{-4}
0.25	No steps	a, b	1	1	0.095 74	0.195 01
	Add steps to all	a	1.010 59	0.999 51	0.101 19	0.199 19
		b	1.010 32	0.999 77	0.100 69	0.199 06
		Error	−0.000 27	0.000 26	−0.005 22	−0.000 67

Table 3 Accuracy while W_{fa} being changed at $H=12$ km, $Ma=1.5$

$Pla/(°)$	Condition	Model	Fr	$sfcr$	SMf	SMc
90	No steps	a, b	1	1	0.290 91	0.203 22
	$W_{fa}(+1\%)$	a	1.003 16	1.002 52	0.288 08	0.203 30
		b	1.003 24	1.002 44	0.287 99	0.203 47
		Error	8.00×10^{-5}	-8.00×10^{-5}	-3.09×10^{-4}	8.37×10^{-4}
100	No steps	a, b	1	1	0.290 93	0.203 23
	$W_{fa}(+1\%)$	a	1.003 83	1.003 39	0.286 95	0.203 33
		b	1.004 00	1.003 21	0.286 71	0.203 58
		Error	0.000 17	-1.80×10^{-4}	−0.000 82	0.001 23

2 APPLICATION OF HYBRID AERO-ENGINE MODEL AND SQP FOR IFPOC

2.1 Linear search SQP algorithm

The problem to be solved by SQP is expressed as

$$\min f(\boldsymbol{x})$$
$$\text{s.t. } \boldsymbol{G}(\boldsymbol{x}) \geqslant 0 \quad \boldsymbol{H}(\boldsymbol{x}) = 0$$

where $\boldsymbol{G}(\boldsymbol{x})=[g_1(\boldsymbol{x}),\cdots, g_{m_1}(\boldsymbol{x})]^{\mathrm{T}}$, $\boldsymbol{H}(\boldsymbol{x})=[h_{m_1+1}(\boldsymbol{x}),\cdots, h_m(\boldsymbol{x})]^{\mathrm{T}}$, $\boldsymbol{x}=[x_1,\cdots,x_n]^{\mathrm{T}}$.

The main idea of SQP algorithm[7] is to solve the following Lagrangian function with two-order approximation, a quadratic regulator (QP) sub-problem

$$L(\boldsymbol{x},\lambda) = f(\boldsymbol{x}) + \sum_{i=1}^{m}\lambda_i g_i(\boldsymbol{x})$$

Firstly, at the iterative point x_k, construct a QP sub-problem. Secondly, take the solution of the sub-problem as the direction $\boldsymbol{d}_k$ of linear search. Finally, repeat $x_{k+1}=x_k+a_k\boldsymbol{d}_k$ (a_k is the kth steplength obtained by linear search) until the optimal solution is achieved. In addition, two-order calibration steplength $\boldsymbol{d}_k^c$ is adopted to overcome Marotos effect.

The realization of SQP algorithm mainly consists of three steps: (1) To renew Hessian matrix of Lagrangian function by BFGS, i.e. $\boldsymbol{B}_k$, (2) To solve the QP sub-problem, (3) To linearly search and calculate the target value. Therefore, through linearizing nonlinear constraint problem, QP sub-problem is described as follows.

Objective function

$$\min \frac{1}{2}\boldsymbol{d}^{\mathrm{T}}\boldsymbol{B}_k\boldsymbol{d} + \nabla f(x_k)^{\mathrm{T}}\boldsymbol{d}$$

Constraint function

$$\nabla \boldsymbol{G}(x_k)^{\mathrm{T}}\boldsymbol{d} + \boldsymbol{G}(x_k) \geqslant 0$$
$$\nabla \boldsymbol{H}(x_k)^{\mathrm{T}}\boldsymbol{d} + \boldsymbol{H}(x_k) = 0$$

where $\boldsymbol{d}=\boldsymbol{d}_k+\boldsymbol{d}_k^c$. And then the problem is solved by QP algorithm.

2.2 Optimization of IFPOC system

The optimization of IFPOC is shown in Fig 3 schematically. This system consists of two levels as host computer and slave computer. The host compute is to simulate the real system, and the slave computer is for real-time tracking and PSC. In Fig. 3, "1" and "2" represent the inputs and outputs of the hybrid aero-engine model respectively, "3" the correct value of aero-engine control variable after optimizing.

In the slave computer, instead of the complicated nonlinear aero-engine model, the hybrid model combined with SQP algorithm is used in optimal control to improve aircraft flight performance and real-time capability.

PSC contains the maximum thrust mode (max F) and the minimum fuel-consumption mode (min sfc). The former is designed to maximize thrust for climbing and accelerating flight. The latter is to minimize fuel flow while maintaining constant F during cruise flight. The operation point of engine is optimized online by adjustingthe aero-engine control variables based on SQP algorithm. Max F and min sfc are mathematically described as

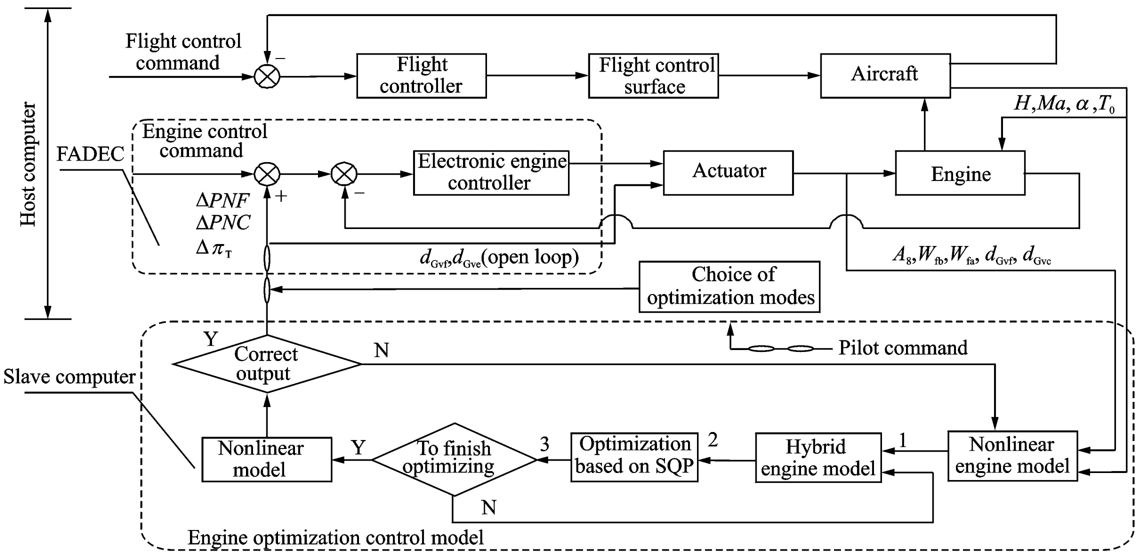

Fig. 3 Schematic diagram of optimal control

$$\max F(\min sfc)$$

$$\text{s.t.}\begin{cases} \boldsymbol{u} = [A_8, W_{\text{fb}}, W_{\text{fa}}, d_{\text{Gvf}}, d_{\text{Gvc}}]^{\text{T}} \\ u_{i,\min} \leqslant u_i \leqslant u_{i,\max} \quad i = 1,\cdots,5 \\ T_{46} \leqslant t_{46\max} \\ pnf_{\min} \leqslant PNF \leqslant pnf_{\max} \\ smf_{\min} \leqslant SMf \\ smc_{\min} \leqslant SMc \\ pnc_{\min} \leqslant PNC \leqslant pnc_{\max} \\ F = \text{const (for min } sfc) \end{cases}$$

3 SIMULATION AND ANALYSIS

The simulation consists of three parts. The first part is the cruise simulation with the minimum fuel mode, the second is the acceleration simulation with the maximum thrust mode, and the third is the optimization time comparison between hybrid aero-engine model and nonlinear aero-engine model. The simulation results are discussed in the following subsections.

3.1 Cruise with minimum fuel-consumption mode

By controlling A_8, W_{fb}, d_{Gvf} and d_{Gvc}, the minimum fuel mode minimizes total engine fuel flow while maintaining constant F during cruise flight. The minimum fuel mode is evaluated at a flight condition of 0.88 Mach and 12 km altitude. Fig. 4 presents the simulation results at the cruise operation point.

According to Fig. 4, the fuel reduction at constant thrust is achieved by opening fan and compressor variable vanes and adjusting A_8. And with the minimum fuel mode, the steady-state value of sfc decreases by 0.65%. In addition, T_{46} decreases by 1.1%. PNF and PNC stays within 2% of the initial values after PSC is engaged.

3.2 Acceleration with maximum thrust mode

Aircraft acceleration performance is essential to accelerating flight. The maximum thrust mode is designed to maximize F and improve aircraft acceleration performance. Fig. 5 shows the simulation results of accelerating at 10 km altitude and 0.7 Mach.

According to Fig. 5, the thrust increases and the flight speed is improved markedly when PSC is applied. Compared with normal acceleration condition, IFPOC system can keep a faster flight speed with the maximum thrust mode and fullfill the flying mission better. In this example, flight speed is raised from 209.6 to 280 m/s, which cost 89.82 s without PSC while 75.18 s with the maximum thrust mode. The acceleration time is shortened by 16.3%, and the average thrust increases by 9.3%.

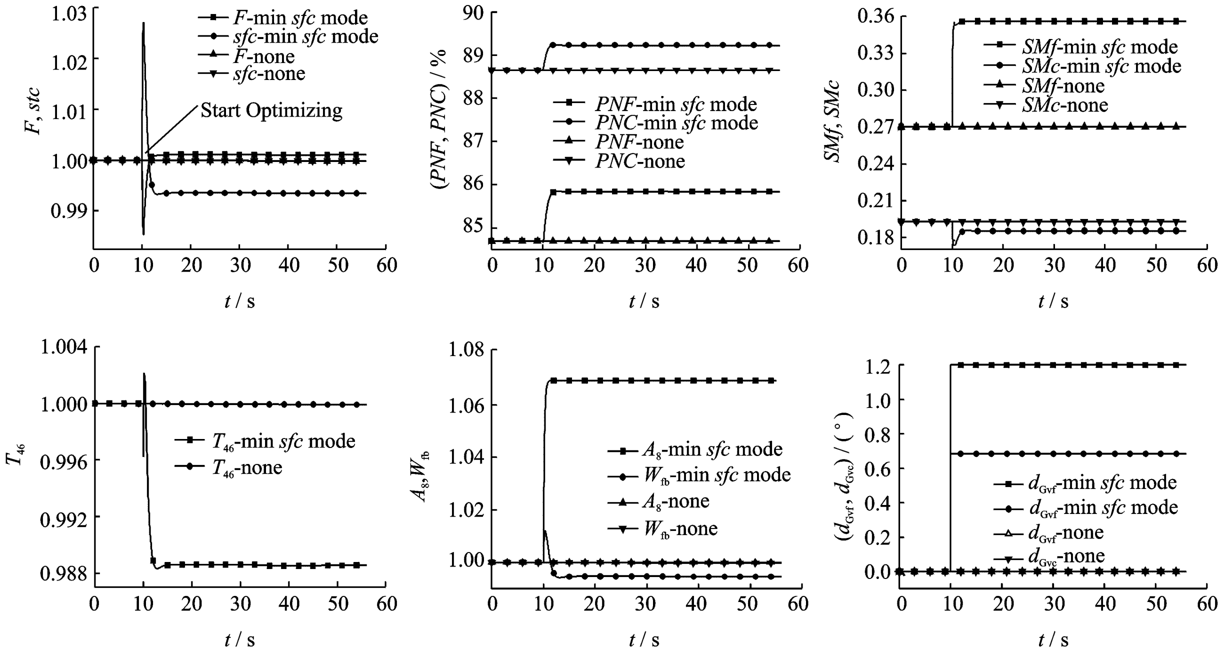

Fig. 4 Cruise at $H=12$ km, $Ma=0.88$ with the minimum fuel mode

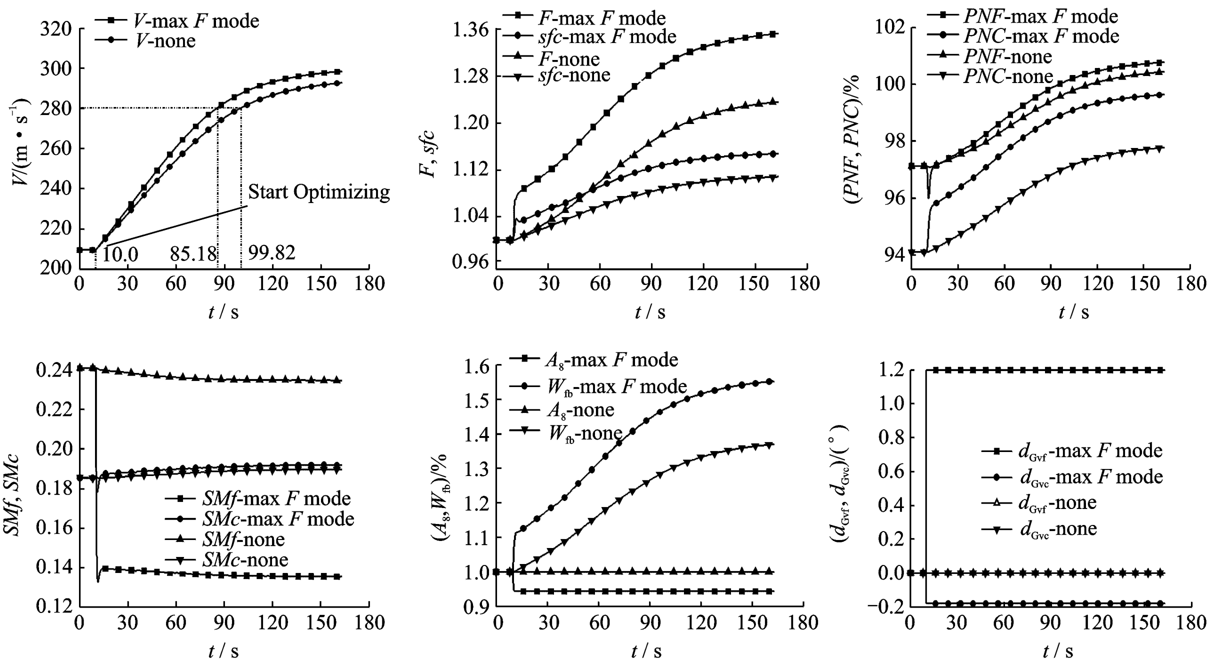

Fig. 5 Acceleration at $H=10$ km and $Ma=0.7$ with maximum thrust mode

3.3 Comparison of optimization time

Through the above simulations, flight performance is improved dramatically after combining the hybrid aero-engine model with SQP in PSC. Meanwhile, the aero-engine does not lead to over-speed, over-temperature and surge. In Table 4, the optimization time based on the hybrid aero-engine model is compared with that of the nonlinear aero-engine model.

According to Table 4, optimization time decreases a lot by using the hybrid aero-engine model in PSC. In IFPOC system, the real-time ability of optimization obtains a ten fold increase with the maximum thrust mode, and more than 20-fold with the minimum fuel mode.

Table 4 Comparison of optimization time

Flight condition	Optimization mode	Optimization algorithm	Optimization time/s	
			Nonlinear model	Hybrid model
Cruise at $H=12$ km and $Ma=0.88$	Minimum fuel mode	SQP	13.133	0.531
Acceleration at $H=10$ km and $Ma=0.7$	Maximum thrust mode	SQP	5.782	0.625

4 CONCLUSION

A steady-state hybrid aero-engine model is built in the whole flight envelope combined with SQP in IFPOC. This approach has two merits. One is to enhance real-time ability of optimization with the hybrid aero-engine model, and the other is to improve optimization accuracy with SQP algorithm. The simulation results shows that the optimal control based on onboard hybrid aero-engine model and SQP can improve real-time capability considerably with satisfactory optimization effectiveness. The proposed method has a great potential in engineering application.

References:

[1] Sun J, Vasilyev V, Ilyasov B. Advanced multivariable control system of aeroengines[M]. Beijing: Beijing University of Aeronautics and Astronautics Press, 2005:557-610.

[2] Gilyard G B, Orme J S. Performance-seeking control: program overview and future directions[J]. NASA Technical Memorandum, 1993, 4531: 593-609.

[3] Orme J S, Conners T R. Supersonic flight test result of a performance seeking control algorithm on a NASA F-15 aircraft[C]//30th AIAA/ASME/SAE/ASEE Joint Propulsion Conference. Indianapolis:AIAA,1994:1-19.

[4] Burcham F W Jr, Haering E A. Highly integrated digital engine control system on an F-15 airplane [C]//AIAA/SAE/ASME, 20th Joint Propulsion Conference. Cincinnati:AIAA,1984:1-10.

[5] Mueller F D. Dual engine application of the performance seeking control algorithm[C]// AIAA/SAE/ASME/ASEE/29th Joint Propulsion Conference and Exhibit. Montery:AIAA, 1993:1-12.

[6] Mathioudakis K, Kamboukos P, Stamatis A. Turbofan performance deterioration tracking using nonlinear models and optimization techniques [J]. Jouranl of Turbomachinery, Transaction of ASME, 2002,124:580-587.

[7] Sun F, Sun J. Aero-engine performance seeking control based on sequential quadratic programming algorithm[J]. Journal of Aerospace Power, 2005,20(5): 862-867. (in Chinese)

[8] Shang Y. Aero gas turbine engines[M]. Beijing: Aviation Industry Press, 1995:110-132. (in Chinese)

[9] Yang G, Sun J, Li Q. Augmented LQR method for aeroengine control systems[J]. Journal of Aerospace Power, 2004, 19(1): 153-158. (in Chinese)

[10] Yao W, Sun J. Online optimization for Turbo shaft engines based on variable inlet guide vane[J]. Journal of Aerospace Power, 2007,22 (11):1930-1934. (in Chinese)

发动机复合模型及其在飞/推综合优化控制中的应用

王健康 张海波 孙健国 李永进

(南京航空航天大学能源与动力学院,南京,210016,中国)

摘要:研究了飞/推综合控制系统的在线优化实时性问题。提出将机载发动机复合模型与序列二次规划(Sequential quadratic programming, SQP)算法结合应用于飞/推综合优化控制的策略。首先,设计适用于全包线范围并可大幅度缩短优化时间的发动机稳态复合模型,然后基于SQP算法将该模型应用到发动机性能寻优控制中,包括最大推力和最小油耗优化模式,从而更加有效地完成各种不同的飞行任务。通过飞机巡航、平飞加速等仿真实验,表明了该优化控制方案能够在具有较好优化效果的前提下,明显提高飞/推综合控制系统的优化实时性。

关键词:飞/推综合优化控制;航空发动机;复合模型;性能寻优控制;序列二次规划

中图分类号:V231

(Executive editor: Zhang Bei)

基金项目:航空科学基金(2010ZB52011)资助项目;江苏省研究生创新培养工程(CXLX11-0213)资助项目;南京航空航天大学基本科研业务费专项科研(NS2010055)资助项目。